BNL-49579
Conf-9310204--8

Submitted to Beam Instrumentation Workshop
Los Alamos National Lab., Los Alamos NM
October 20-23, 1993

SIGNAL GENERATION IN GAS DETECTORS*

Arnold Stillman
Brookhaven National Laboratory, Upton, NY 11973

ABSTRACT

This tutorial describes the generation of electrical signals in gas detectors. Ionization of the gas by the passage of charged particles generates these signals. Starting with the Bethe-Bloch equation, the treatment is a general introduction to the production of ion-pairs in gas devices. I continue with the characterization of the ionization as an electrical signal, and calculate the signal current in a simple example. Another example demonstrates the effect of space charge on the design of a detector. The AGS Booster ionization profile monitor is a model for this calculation.

Introduction

When a charged particle passes through matter, it deposits energy in several ways. This is true for solids, liquids and gases, but I shall stick to describing only the interactions in gases, since gas detectors are among the commonest of detectors in beam line engineering. Liquid and solid particle detectors are mainly for experimental data-taking purposes and are beyond the scope of this discussion. In gas detectors, the charged particle deposits energy according to how much instantaneous energy it has along its path in the gas volume. The interactions that occur for low energy particles are much different than the high energy, relativistic interactions. In most practical applications, particle energies are moderately relativistic, and these energies will be the ones of interest here.

The incident particle can suffer three main types of collisions with gas molecules: inelastic ionizing events, inelastic non-ionizing events, and elastic collisions. The elastic collisions are of no concern, they are simply billiard-ball type collisions that do not create ion pairs. Similarly, inelastic non-ionizing events do not create ion pairs, but we shall see that they do effect the analysis of ionizing events. The inelastic collisions that produce ion pairs are the real subject of detector engineering. In these events, an energetic particle, which can be an electron, an ion, or an exotic particle like a pion or muon, scrubs off energy by separating electrons bound to gas atoms from the nuclei of those atoms. Most of the ionization that occurs removes only the outer shell, valence electrons from the atom, but there is a finite probability for the removal of more strongly bound electrons. It is pretty small though, for the commonest beam energies at accelerators. Of course, the incident particle often has enough energy to undergo

*Work performed under the auspices of the U.S. Department of Energy, Contract No. DE-AC02-76CH00016.

several of these ionizing collisions, losing some fraction of its energy with each one. Thus the particle generates a train of ion/electron pairs, called simply ion pairs, along its path through the gas. These pairs will drift or diffuse in the gas, depending on the gas pressure, and form a current that becomes the detector signal.

Ionization in Gases

The ionization of gases by the passage of charged particles depends somewhat on the nature of the incident particle. Generally, electrons behave differently from other charged particles (except possibly positrons) in generating ion pairs. Also remember that the ionization is different for relativistic and non-relativistic particles. It is probably best to consider the most common situation, that of relativistic ions passing through a certain gas volume.

Ions of moderately relativistic velocities (that is, ions with $\beta \gtrsim \alpha$, where β is v/c, v is the particle velocity, c is the speed of light, and $\alpha \approx 1/137$ is the fine structure constant, $e^2/\hbar c$, in which e is the magnitude of the elementary charge and $\hbar$ is Planck's constant) lose energy mainly through ionization events. At these velocities, the ion velocity is of the order of the average velocity of the outer shell electrons in the gas molecules. Up to $\beta \approx .8$ or .9, the Bethe-Bloch equation[1] determines the mean rate of energy deposition;

$$-\frac{dE}{dx} = 4\pi N_A r_e^2 m_e c^2 z^2 \frac{Z}{A}\frac{1}{\beta^2}\left[ln\left(\frac{2m_e c^2\gamma^2\beta^2}{I}\right) - \beta^2 - \frac{\delta}{2}\right]. \qquad (1)$$

Here, the charge of the incident particle is ze, the atomic number of the atoms of the gas is Z, their atomic weight A. Note that the specific value of the elementary charge, e, does not enter into Eq. 1, only the number of them z, does. The other variables are m_e and r_e, the mass and classical radius of the electron, N_A, Avogadro's number, I a catch-all ionization constant that depends on the gas, and δ, a term that attempts to account for shielding of the incident particle's electric field by the atomic electrons of the medium. The energy loss, dE/dx, includes energy lost to all processes, ionizing and non-ionizing. The Beth-Bloch equation looks rather imposing, but splitting off the various terms and analyzing them individually is not too difficult.

Before continuing to examine the terms in the Bethe-Bloch equation, however, it is necessary to describe the units of dE/dx. When a charged particle loses energy along a path in the gas, the rate of energy loss should depend on the density of the gas. This dependence simply reflects the fact that there is more energy loss for a speeding particle if there are more molecules in its way. It is natural, then, that the differential variable dx be a measure of the density-weighted path through the gas. Thus the units of dx are in mass per unit area, generally g cm^{-2}. It is important not to confuse this dx with a differential linear *distance*. Unfortunately, the notation does nothing to eliminate the confusion, though it is the standard notation. The units of the Bethe-Bloch equation are therefore energy per mass per unit area, usually expressed in eV cm^2 g^{-1}.

The factor $4\pi N_A r_e^2 m_e c^2$ equals .3071 MeV cm^2 g^{-1} and the factor $2m_e c^2$ is 1022 MeV. Plugging the numerical values into the equation gives a form more tractable for numerical calculations;

$$-\frac{dE}{dx} = .3071 z^2 \frac{Z}{A}\frac{1}{\beta^2}\left[\ln\left(\frac{1022\gamma^2\beta^2}{I}\right) - \beta^2 - \frac{\delta}{2}\right] \left(\text{MeV cm}^2/\text{g}\right) \qquad (2)$$

This form also makes examining the individual terms easier. Equation 1 is precise only to a few percent, often to little better than 10%; it is these individual terms that cause the imprecision. For instance, the ionization constant I has a dependence on Z reliable to about 10%. It is roughly $I = 16Z^{.9}$ eV. The constant δ depends on the charge density of the medium, which increases with the mass density of the medium, and in fact, represents the *density effect.* As more electrons occur beside the path of the incident particle, more electric screening of the incident particle's electric field occurs. This screening attenuates the effect of the relativistic, transverse electric field that causes ionization.

In many materials, *i.e.* for various Z values, there is a broad minimum in dE/dx. Particles with values of β in this range generate a minimum of ion pairs along their path. These are *minimum ionizing particles*, often abbreviated mips. There is a difference, though, between energy lost by the incident particle and the number of ion pairs that the lost energy produces. The amount of energy to create ion pairs varies both with incident particle type and gas species. It is incorrect to assume, for instance, that 13.6 eV of energy, the ionization energy of hydrogen, produces an ion pair (*i.e.* a proton and an electron) when deposited by a charged particle in pure hydrogen gas. Let us first finish examining the Bethe-Bloch equation before continuing on to the complicated nature of ion pair creation in gases.

The factor multiplying the square brackets, $.3071 z^2 \frac{Z}{A}\frac{1}{\beta^2}$, decreases as $1/\text{velocity}^2$, so for low velocity particles, the ionization increases. A classical way to think about the low velocity enhancement is to imagine the electric forces between the target atom's bound electron and the incident particle charge. At low velocities, the two charges have an interaction time that increases the probability for ionization. The forces are in play for a significant amount of time. At high velocities, the reverse is true, and the particle zips by the atom or molecule, just nudging the electron orbit, but not destroying it. This classical picture is not quite true in a strict quantum mechanical sense, but it is useful in understanding the dependence of the ionization on incident particle *velocity* rather than *energy.* At very low incident velocities, though, charge exhange interactions and quantum mechanical effects completely pervert the simple ionization picture. Luckily, these velocities are too low to be of interest to radiation detector designers.

The bracketed factor, $\ln\left(\frac{1022\gamma^2\beta^2}{I}\right) - \beta^2 - \frac{\delta}{2}$, depends somewhat on the density factor δ, but almost universally rises, first as $2\ln\gamma$, then as $\ln\gamma$. This relativistic rise in dE/dx also has a simple "classical" argument that allows one to visualize the underlying physics. When the incident particle has a large velocity, a velocity significant with c, its increase in inertia appears to the target atoms as an increase of mass. In the frame of the gas atoms, *i.e.*the lab frame, the absolute energy loss is rather high, though the

fractional amount the incident particle gives up to the gas may be actually rather low.

However, not all of the energy lost by the incident particle contributes to the creation of ion pairs. Some energy gets lost to processes other than ionization. In monoatomic gases, these processes are few; the important ones are mainly the creation of excited atomic states. It is a different situation in molecular targets, though. These are gases such as CO_2, CO and others that are common in detectors. These gases have molecular excitations, such as rotational and vibrational modes, which absorb energy strongly at certain frequencies. There are ways to quantify the contributions of these effects to the total energy loss. Each available mode has an oscillator strength, f_i associated with its excitation energy, ϵ_i. The sum

$$\ln \epsilon_t = \sum_i f_i \ln \epsilon_i \tag{3}$$

determines a total amount of energy ϵ_t lost to these processes.

The difficulty in estimating ϵ_t for any particular target gas lies in knowing the values of the oscillator strengths. This is a very complicated bookeeping problem for real situations. The best way to approach the problem is to make use of the empirical values of the gap between total energy lost and energy lost to ionization. The Appendix is a tabulation of this energy deficit for various gases, incident particles, and incident particle energies.

Signal Estimation

To clarify the ion-pair production concepts, it will be useful to estimate the signal in a prototypical detector. In no way would this simple example be reflective of real devices, but it is still instructive. Suppose a chamber, filled with an Argon/CO_2 mixture of 90% Argon and 10% CO_2, that is 10 cm long and has an aperture wider than the size of the beam. Now let us shoot a proton beam through the gas and put a bias voltage across some electrodes to collect the ion pairs. Assume further that the chamber geometry is quite simple, just two plates parallel to the beam direction. The beam passes midway between them, as Fig. 1 shows.

We can now estimate the signal current that a 2 GeV beam of 10^6 protons would produce when it passes through the chamber once. The first calculation is that of the two gas densities, since they will be necessary to convert the reduced distance to linear distance. Using the law of partial pressures, here written as,

$$\frac{1}{RT} \sum_i P_i = \sum_i \rho_i, \tag{4}$$

where P_i is the partial pressure of each species i (in this case, $i = 1, 2$), gives the molar density ρ_i for each component of the gas. The partial pressures of the gases sum to the total pressure in the chamber, so $P_1 = .9 \times 760 = 684$ Torr and $P_2 = .1 \times 760 = 76$ Torr. Inserting the gas constant $R = 62400$ Torr cm^3/K and the absolute temperature,

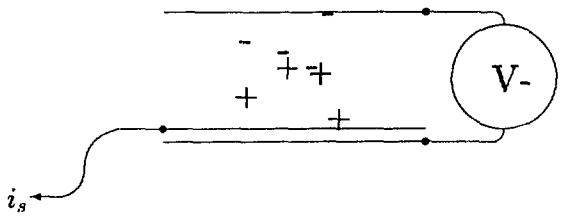

Figure 1: A Simple Chamber Model. The electrodes above and below provide the collection field. The ions drift downward to the anode to form the electronic signal.

300 K, into Eq. 4 gives $\rho_1 = 36.5 \times 10^{-6}$ mole cm^{-3} for the Ar and $\rho_2 = 4.06 \times 10^{-6}$ mole cm^{-3} for the CO_2 molar densities. The mass densities are the mole densities times the molecular weights of the component gases, so $\rho_1 = 36.5 \times 10^{-6}$ mole cm$^{-3}\times$ 40 g mole^{-1} $= 1.46\times10^{-3}$ g cm^{-3} and $\rho_2 = 4.1\times10^{-6}$ mole cm$^{-3}\times$ 44 g mole^{-1} $= .179\times10^{-3}$ g cm^{-3} are the mass densities. It is now simple to substitute the densities into the equation for the energy loss,

$$\frac{dE}{dx} = \frac{1}{\rho}\frac{dE}{dl}, \tag{5}$$

where dl is now the distance along the path of the incident protons. Using the values from the Appendix, dE/dx for Ar and 2 GeV protons is 1.47 MeV/g cm^2 , and dE/dx for CO_2 is 1.62 MeV/g cm^2. Dividing these numbers for the energy loss by the energy required to produce a single ion pair, W_i, gives the number of ion pairs per cm for each gas. W_i for Ar is 26 eV/pair, and W_i for CO_2 is 33 eV per pair. So finally, the total number of ion pairs produced along the proton path is

$$N_I = 10\left[\frac{1}{26}(1.46\times10^{-3})(1.47\times10^{6}) + \frac{1}{33}(.179\times10^{-3})(1.62\times10^{6})\right] \text{ ion pairs,} \tag{6}$$

or, $N_I \approx 913$ ion pairs. To get the total ion pair production, we must multiply the number of ion pairs per proton by the number of protons in the beam. If the beam is a circulating beam, we must also multiply by the revolution frequency to get the ion pair production per second, which is a current. In this example, it is

$$i_s = 10^6 e N_I f \tag{7}$$

where f is the revolution frequency. For a revolution frequency of 4.0 MHz, $i_s \approx .58$ mA. If this chamber were in a linear accelerator, there would be no revolution frequency;

rather the proton current would simply be i_{beam}/e and the signal would be

$$i_s = \frac{i_{beam}}{e} N_I. \tag{8}$$

However, i_{beam} must also include duty cycle corrections.

Signal Collection

In all gas radiation detectors, macroscopic electromagnetic fields collect the ion pairs by causing either the ions or electrons to drift to one or more anodes. Of course, the collection fields collect both positive and negative charges, but the source of the collection field, the bias source, usually has a low enough impedance that the small current flowing onto the bias electrode induces only negligible changes in the bias voltage. The shape of the collection fields can often be important for segmented anode chambers, but for loss monitors and ion chambers that monitor total beam current, the shape and magnitude of the fields serve only collect the total ion current. These considerations deserve further discussion, though.

Let us contrast two types of detector that collect the total ionization current in their fiducial volume, the gas volume through which the incident particle creates *collectible* ion pairs. The first type of detector is a coaxial chamber, a cylindrical electrode around a gas volume with a thin wire in the center. The whole assembly has cylindrical symmetry, and the central wire is thin, so that this type of chamber has an inherent gain associated with the ion collection. Ref. [2] describes the gain process, pointing out that essentially all the gain occurs in a small sheath around the central wire. For this geometry, the ion pairs have no escape from the collecting electrodes, since the fiducial volume is within a cylinder. Suppose, however, the geometry of an ion chamber, the second type of detector. This geometry is that of a parallel plate capacitor, with one plate serving as the signal collection node and the other the bias field electrode. Ion pairs produced near the edges of the plates have an opportunity to escape, if there is a low enough collecting field. In practice, this is never the case, since the ion chamber would always present a face to the beam much greater than the beam width. It is apparent though, that there can be some constraints on the magnitude of the collecting fields, *i.e.* the bias voltage.

This signal dependence on collection field is nowhere greater than in segmented anode detectors. Examples of these detectors are wire chambers through which the beam actually passes, and non-invasive detectors, which sit outside the beam aperture. To understand the effects of collection fields on the signals from these detectors, it is important to remember that these detectors exist to provide beam profile information, not simply intensity measurements. Thus, shape preservation of the beam-induced ion current is of primary importance. In wire chambers that sit in the beam, the bias field imperfections cause the most drastic shape distortions. In non-invasive detectors, the bias field errors combine with the effects of beam space charge to distort shape information. The space charge effect of the ion pair current is a little more complicated, but much less intense.

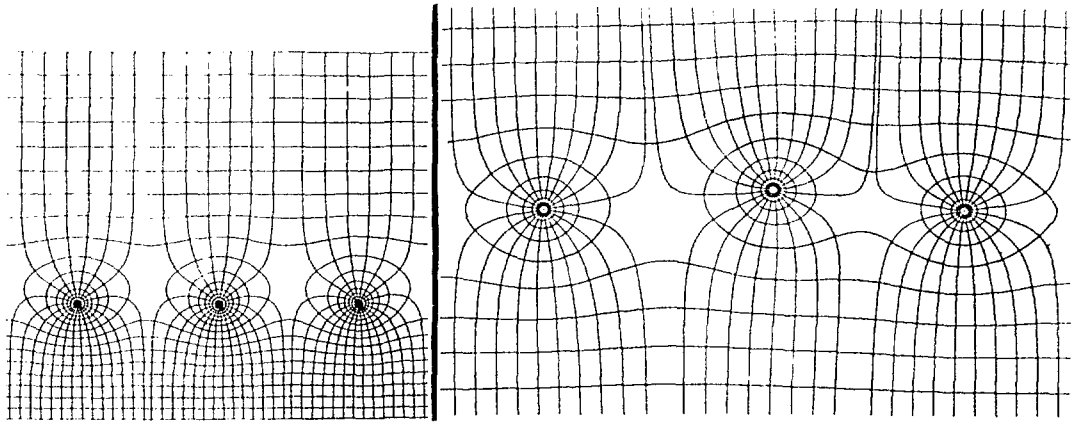

Figure 2: Field lines around the wires of a typical wire chamber. **a.** The distance from the wires to the bias planes is unequal, causing a change in the field strengths above and below the wire plane. **b.** An offset in the position of one of the wires produces a distortion in the collection field region.

Some examples of wire chamber field lines are in Fig. 2 [3]. In the first figure, the collection regions above and below the wire plane have different field strengths. Since the beam passes through both regions equally, (its motion is vertical in this view) the differences have no effect. However, in Fig. 2b., the distortion in shape can cause distortions in the profile information. Notice that a particle that passes between the offset wire and one of the normal wires will generate a signal that will not split correctly between the wires. Suppose, for instance, that the particle passes exactly halfway between the left and middle wires in Fig. 2b. The field lines in this region cause signal current to drift preferentially to the central wire. But the correct signal would be one that splits evenly between the two wires. The position information thus becomes distorted. The wire spacing in real chambers is on the order of millimeters, so one might think the error to be trivial. It is not, though. The profile information from a multi-wire detector is the input to a curve fitting algorithm. If the profile should be Gaussian, for instance, and a 32-channel wire chamber yields as many valid data points for the fit, *the spatial resolution of the wire chamber is much finer than the wire pitch.* How much finer is a question of the goodness of the fit, but rarely is it worse than half the wire spacing.

Examining the design of a non-invasive residual gas detector will afford an opportunity to discuss beam space charge effects that are not present in invasive wire chamber devices. The Brookhaven Booster ionization profile monitor[4] is a profile monitor whose collecting anodes sit outside the beam aperture. It relies on the ionization of whatever residual gas is in the beam line (probably H_2 and CO) to generate signal currents. The proton beam in the Booster can be intense enough, though, to have significant space charge effects on the profiles. Estimating these space charge effects will have repercussions on many aspects of the design of the IPM. Fig. 3 is a schematic drawing of the geometry, showing the proton beam emerging from the plane of the page, and ions and

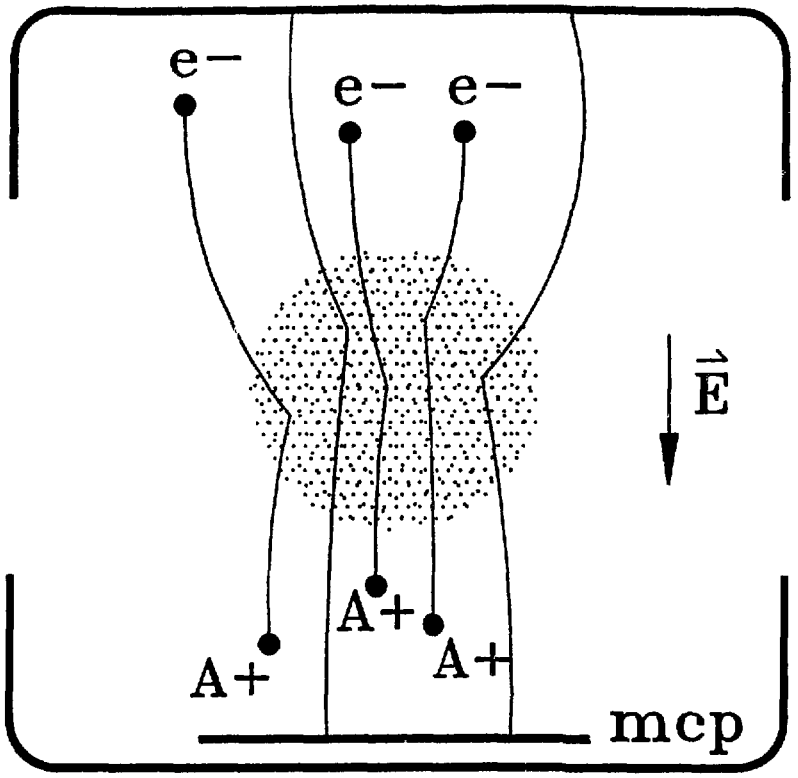

Figure 3: Ion Pairs in Profile Monitor. A^+ indicates an ion, and e^- an electron. The ion pairs drift along the direction of $\vec{E}$; mcp denotes a microchannel plate detector, and the curved thick lines are the collection electrodes.

electrons drifting under the influence of space charge and collecting fields. To estimate the space charge electric field, it is necessary to determine the charge density of the beam. The circulating proton beam is an average current,

$$I = Nef \tag{9}$$

where N is the number of protons in the beam (composed of three bunches), e is the elementary charge, and f is the revolution frequency. The charge density that makes up this average current is a two-dimensional Gaussian distribution of charges multiplied by the linear charge distribution along the circumference of the ring;

$$\rho(x, y, z) = \rho(z) e^{-x^2/2\sigma_x^2} e^{-y^2/2\sigma_y^2}, \tag{10}$$

where $\rho(z)$ is the normalized linear charge density along the beam direction, z. Integrating the charge distribution should give the total number of protons in the beam. It will be easiest to integrate over only one turn in the machine, and then multiply by the revolution frequency to confirm the current in Eq. 9. Thus,

$$I = f\rho(z) \int_V e^{-x^2/2\sigma_x^2} e^{-y^2/2\sigma_y^2}\, dx\, dy\, dz, \tag{11}$$

or, assuming $\sigma_x = \sigma_y = \sigma$ and switching to cylindrical coordinates,

$$I = f\rho(z) \int e^{-r^2/2\sigma^2}\, r dr\, d\theta\, dz, \tag{12}$$

where r is the radial distance from the nominal beam center, θ is the azimuthal angle around this point, and z is the longitudinal distance, which will integrate to the circumference of the Booster. The fact that the variable z is not the distance along a straight line will not make a difference in this approximation. Remember also that the area integral transforms $dxdy$ to rdr. Evaluating the integral and inserting the circumference of the Booster as $2\pi R$ gives

$$I = (2\pi\sigma)^2 R f \rho(z). \tag{13}$$

To determine the space charge field, apply Gauss' Law,

$$\vec{\mathbf{E}} \cdot \mathrm{d}\vec{\mathbf{a}} = 4\pi \mathrm{q} \tag{14}$$

to the charge distribution in the beam, finding that

$$\vec{\mathbf{E}}(\vec{r}) = \frac{4\pi}{2\pi r} q(r)\hat{r}. \tag{15}$$

Determining $q(r)$ is not too difficult. Using the charge distribution in Eq. 12, the amount of charge within a cylinder of radius r' is simply

$$q(r) = \int_0^r \rho(r')\, dr', \tag{16}$$

or,

$$q(r) = \sigma^2(1 - e^{-r^2/2\sigma^2}). \tag{17}$$

producing an electric field,

$$\vec{\mathbf{E}}(\vec{r}) = 2\sigma^2(1 - e^{-r^2/2\sigma^2})\frac{\hat{r}}{r}, \tag{18}$$

which has a maximum for $r/2\sigma^2 \approx 1.121$. This maximum value for the space charge field is the most useful value for estimating the space charge spreading of the beam profile signal. If the channel pitch between anodes is w and the distance from the creation of the ion pair at the beam center line to the anode plane is l, as in Fig. 4, then, at this maximum field point, the ion receives the greatest lateral kick, causing the greatest error in the width measurement. In a time t, the ion drifts a horizontal distance $x = \frac{e}{m} E_{scmax} t^2$, where E_{scmax} is the magnitude of the maximum space charge electric field. In the same time interval, the ion also drifts a vertical distance $l = \frac{e}{m} E_c t^2$ under the influence of the collection field, E_c. Dividing these two equations and setting the radial drift, r, equal to the channel pitch, w, gives [4]

$$w/l = E_{scmax}/E_c. \tag{19}$$

In deriving this equation, I assume that the ion accelerates due to the presence of electric fields. This is not true for gases at atmospheric pressure; the ion actually diffuses at some constant velocity. However, all kinematic effects on velocity or acceleration divide out by taking the ratio of the distances travelled in the two planes.

Equating the channel pitch to the maximum radial drift means that the travel of the ion due to the space charge is below the resolution of the profile monitor, since it is

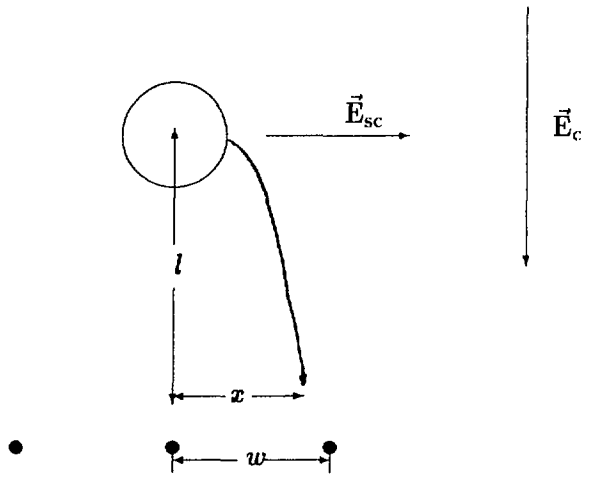

Figure 4: Ion Trajectory. The space charge and collection fields cause an ion from an ion pair to drift to the anode. The circle represents the space charge cloud of the beam, and the filled circles are the anodes.

only over the space occupied by one anode. Thus, the space charge effect of the beam relates three separate parameters of the profile monitor design, the collection field, E_c, the channel pitch, w, and the distance of the anode plane from the beam center line, l. The channel pitch and the distance l often are not free variables for the instrument designer, so choosing an acceptable value for E_c constrains the design.

Appendix

Various sources list energy loss tables for gases. The data here are mainly from Ref.[5].

Gas	Z	A	δ	IZ^{-9}	W_i	dE/dx	dE/dl	N_I
H_2	2	2	8.38×10^{-5}	29.9	37	4.03	.34	9.2
He	2	4	1.66×10^{-4}	29.9	41	1.94	0.32	7.8
N_2	14	28	1.17×10^{-3}	172.0	35	1.68	1.96	56
O_2	32	32	1.33×10^{-3}	194.0	31	1.69	2.26	73
Ne	10	20.2	8.39×10^{-4}	127.1	36	1.68	1.41	39
Ar	18	39.9	1.66×10^{-3}	215.7	26	1.47	2.44	94
Kr	36	83.8	3.49×10^{-3}	402.5	24	1.32	4.60	192
Xe	54	131.3	5.49×10^{-3}	579.8	22	1.23	6.76	307
CO_2	22	44	1.86×10^{-3}	258.4	33	1.62	3.01	91
CH_4	10	16	6.70×10^{-4}	127.1	28	2.21	1.48	53
C_4H_{10}	34	16	2.42×10^{-3}	382.3	23	1.86	4.50	195

KEY

Z=Atomic Number
A=Atomic Weight
δ, IZ^{-9}, and W_i are in eV.
dE/dx and dE/dl are in Mev/g cm^{-2} and keV/cm, respectively.
N_I is in ion pairs/cm.

References

[1] U. Fano, Ann. Rev. Nucl. Sci. **13** , 1 (1963).

[2] M. Johnson, in AIP Conference Proceedings 212, Accelerator Instrumentation, edited by Edward R. Beadle and Vincent J. Castillo (American Institute of Physics, New York, 1990), pp. 165-173.

[3] G. A. Erskine, Nucl. Instrum. Methods, **105** ,565 (1972).

[4] A. N. Stillman, R. Thern, and R. L. Witkover, Review of Scientific Instruments, **63 (6)** , 3412 (1992).

[5] F.Sauli, CERN Report No. 77-09, 1977.